Evaluation of the Algorithms and Parameterizations for Ground Thawing and Freezing Simulation in Permafrost Regions

Yinsou Zhang
Carleton University

Sean K. Carey
Carleton University

William L. Quinton
Wilfrid Laurier University, wquinton@wlu.ca

Evaluation of the algorithms and parameterizations for ground thawing and freezing simulation in permafrost regions

Yinsuo Zhang,[1] Sean K. Carey,[1] and William L. Quinton[2]

[1] Ground thawing and freezing depths (GTFDs) strongly influence the hydrology and energy balances of permafrost regions. Current methods to simulate GTFD differ in algorithm type, soil parameterization, representation of latent heat, and unfrozen water content. In this study, five algorithms (one semiempirical, two analytical, and two numerical), three soil thermal conductivity parameterizations, and three unfrozen water parameterizations were evaluated against detailed field measurements at four field sites in Canada's discontinuous permafrost region. Key findings include: (1) de Vries' parameterization is recommended to determine the thermal conductivity in permafrost soils; (2) the three unfrozen water parameterization methods exhibited little difference in terms of GTFD simulations, yet the segmented linear function is the simplest to be implemented; (3) the semiempirical algorithm reasonably simulates thawing at permafrost sites and freezing at seasonal frost sites with site-specific calibration. However, large interannual and intersite variations in calibration coefficients limit its applicability for dynamic analysis; (4) when driven by surface forcing, analytical algorithms performed marginally better than the semiempirical algorithm. The inclusion of bottom forcing improved analytical algorithm performance, yet their results were still poor compared with those achieved by numerical algorithms; (5) when supplied with the optimal inputs, soil parameterizations, and model configurations, the numerical algorithm with latent heat treated as an apparent heat capacity achieved the best GTFD simulations among all algorithms at all sites. Replacing the observed bottom temperature with a zero heat flux boundary condition did not significantly reduce simulation accuracy, while assuming a saturated profile caused large errors at several sites.

1. Introduction

[2] Approximately 35% of the earth's surface is subject to seasonal freezing and thawing, with 26% estimated to be underlain with permafrost [*Williams and Smith*, 1989]. Because the thermal and hydraulic properties of frozen soils are distinct from those of the same soil in the unfrozen state [*Lachenbruch et al.*, 1982; *Farouki*, 1986; *McCauley et al.*, 2002; *Quinton et al.*, 2005; *Overduin et al.*, 2006], ground thawing and freezing processes strongly influence the surface energy balance and hydrological processes [*Woo*, 1986; *Williams and Smith*, 1989]. The latent energy consumed (released) during thawing (freezing), along with changes in soil thermal properties, greatly alters the surface and subsurface energy partitioning patterns during the unfrozen, frozen and transition periods in permafrost soil [*Boike et al.*, 1988; *Gu et al.*, 2005; *Quinton et al.*, 2005]. In

permafrost-dominated watersheds, snowmelt is typically a considerable portion of water inputs [*Woo*, 1986; *McNamara et al.*, 1998; *Carey and Woo*, 1999]. Infiltration and redistribution of meltwater are strongly controlled by soil thawing in the active layer due to the impermeable nature of the cryofront and the large vertical changes in soil hydraulic conductivity [*Metcalfe and Buttle*, 1999; *Carey and Woo*, 1999; *Quinton et al.*, 2005]. Given the importance of frozen ground to water and energy cycling near the ground surface, representing ground thawing and freezing depths (GTFD) in land surface models (LSMs) and hydrological models is critically important [*Slater et al.*, 1998; *Pitman et al.*, 1999; *Luo et al.*, 2003; *Yi et al.*, 2006]. Recently, efforts have been made to predict changes to global or regional permafrost in response to changes in climate forcing with comprehensive numerical models including thaw/freeze algorithms [e.g., *Lawrence and Slater*, 2005; *Sushama et al.*, 2006, 2007; *Zhang et al.*, 2007a]. Although climate warming scenarios used by most studies are similar, their predictions differed markedly. *Zhang et al.* [2007a] predicted 16−20% reduction in the permafrost area in Canada between 1999 and the end of 21st century, while *Lawrence and Slater* [2005] predicted 60−90% reduction of the permafrost area globally in about

[1] Department of Geography and Environmental Studies, Carleton University, Ottawa, Ontario, Canada.
[2] Cold Regions Research Centre, Wilfrid Laurier University, Waterloo, Ontario, Canada.

the same period. Large discrepancies in the predictions of future permafrost fate suggests that further examinations of the basic model assumptions and simulation processes including the thawing and freezing are necessary [*Burn and Nelson*, 2006; *Delisle*, 2007; *Nicolsky et al.*, 2007].

[3] Existing algorithms to simulate GTFD vary in the: (1) types of algorithms, (2) parameterizations of soil thermal properties for both frozen and unfrozen soils, (3) parameterizations of unfrozen water content in frozen soil, (4) treatment of latent energy during thawing and freezing, and (5) settings of model configurations such as resolution of time step and soil layers, and the boundary conditions. A brief review of algorithms and parameterizations for GTFD simulation is provided in section 2.

[4] Due largely to logistical difficulties in obtaining sufficient field data in permafrost environments, evaluation of GTFD simulation algorithms and their parameterization techniques remains challenging. Previous studies have prescribed surface forcing [e.g., *Jumikis*, 1977; *Goodrich*, 1978, 1982b; *Lunardini*, 1981; *Riseborough*, 2004], or prescribed soil moisture and thermal properties [e.g., *Goodrich*, 1978, 1982b; *Romanovsky et al.*, 1997; *Hinzman et al.*, 1998; *Li and Koike*, 2003; *Ling and Zhang*, 2004; *Woo et al.*, 2004]. For example, in the validation of a modified Stefan's algorithm, a 5% unfrozen water content was used for six field sites ranged from polar desert to agricultural land [*Woo et al.*, 2004], while observed values ranged from 0% in coarse-grained mineral soil to more than 20% in certain organic or clay soils [*Anderson and Tice*, 1972; *Nakano and Brown*, 1972; *Romanovsky and Osterkamp*, 2000; *Quinton et al.*, 2005; *Overduin et al.*, 2006]. Most existing evaluation/validation studies of GTFD simulations only included single algorithm [e.g., *Goodrich*, 1978; *Fox*, 1992; *Hinkel and Nicholas*, 1995; *Hinzman et al.*, 1998; *Cherkauer and Lettenmaier*, 1999; *Quinton and Gray*, 2001; *Zhang et al.*, 2003; *Woo et al.*, 2004; *Hayashi et al.*, 2007], and only a few compared different algorithms [e.g., *Romanovsky et al.*, 1997; *Luo et al.*, 2003]. Shortcomings of evaluations by *Romanovsky et al.* [1997] and *Luo et al.* [2003] were that the compared models differed in many ways in representing processes related to thawing/freezing. The three numerical models compared by *Romanovsky et al.* [1997] differed in their discretizing techniques (finite difference vs. finite element), in treatments of latent heat during thawing/ freezing and in the parameterization of unfrozen water. The 21 LSMs compared by *Luo et al.* [2003] have even larger diversity in thawing and freezing algorithms, soil thermal and unfrozen water parameterizations, simulations of ground surface temperature, soil moisture and snow depth. While results from these studies enhance awareness of key processes (e.g., unfrozen water, ground surface temperature, snow dynamics, etc.), it is hard to identify reasons for differences in GTFD and subsurface temperature, limiting the applicability of the findings.

[5] To provide a comprehensive evaluation of existing algorithms for GTFD simulations in permafrost regions, this study compared the simulation results of five GTFD algorithms with observations at four locations in two northern watersheds: Scotty Creek, Northwest Territories and Wolf Creek, Yukon Territory, Canada. The five algorithms include a semi-empirical algorithm, two analytical algorithms and two numerical algorithms. For each algorithm, the driving variables and input parameters were obtained from a common set of field observations, or gap-filled from available observations. In addition, three soil thermal conductivity parameterizations, three unfrozen water parameterizations, and two commonly applied parameter prescription methods (i.e., zero heat flux at the bottom of soil column and saturated soil moisture) were examined at the four sites. To ensure that the evaluation results are not disturbed by factors other than those to be evaluated, some model configurations (i.e., resolutions of time step and soil layers, position of lower boundary), were examined prior to the algorithm and parameterization evaluation and the most appropriate sets were applied to each site. Results from this research will provide guidelines for the implementation of appropriate algorithms and parameterization techniques for GTFD simulation in permafrost environments based on the type and quality of available data, the time, and spatial scales of the application.

2. Review of Algorithms, Parameterizations, and Configurations for GTFD Simulation

2.1. Types of Algorithms

[6] There are three categories of GTFD simulation algorithms: empirical and semiempirical, analytical, and numerical. Equations of GTFD simulation used in this study are presented in Table 1. Empirical and semiempirical algorithms relate GTFD to some aspect of surface forcing by one or more experimentally established coefficients [e.g., *Van Wijk*, 1963; *Abbey et al.*, 1978; *Quinton and Gray*, 2001; *Anisimov et al.*, 2002]. Equation (1), referred to as Accumulated Thermal Index Algorithm (ATIA) hereafter, is one of the most commonly used semi-empirical algorithms [*Woo*, 1976; *Nelson and Outcalt*, 1987; *Hinkel and Nicholas*, 1995; *Nelson et al.*, 1997], which is a simplified expression of Stefan's analytical solution (equation (2); *Stefan* [1890], as cited by *Jumikis* [1977]). While no soil parameters are required, the empirical coefficient (β) has to be calibrated with observed GTFD in situ, limiting the spatial and temporal transferability of the method.

[7] Analytical algorithms are specific solutions to heat conduction problems under certain assumptions. The most widely applied analytical solution is Stefan's formulation (equation (2)), which is most applicable in wet homogeneous ground conditions based on the original assumptions [*Carlson*, 1952; *Jumikis*, 1977; *Lunardini*, 1981]. Various modifications have been made to extend its applicability. *Kersten* [1959] developed a scheme for layered soils, while *Woo et al.* [2004] further improved the algorithm by including top and bottom forcing called the Two Directional Stefan Algorithm (TDSA), which can simulate multiple frozen and thaw fronts in layered soil. *Hayashi et al.* [2007] developed a simple analytical equation (equation (3)) to simulate GTFD at a permafrost site with layered peat soil based on similar assumptions in Stefan's original algorithm, and hereafter referred to as Hayashi's Modified Stefan Algorithm (HMSA). Stefan's algorithm and its various modifications have been widely applied to simulate GTFD in permafrost models [e.g., *Carlson*, 1952; *Jumikis*, 1977; *Lunardini*, 1981; *Woo et al.*, 2004; *Carey and Woo*, 2005], hydrological models [e.g., *Fox*, 1992; *Zhang et al.*, 2000], and LSMs [e.g., *Li and Koike*, 2003; *Yi et al.*, 2006].

Table 1. List of Equations

Equations	Number
Semiempirical algorithm	
$Z = \beta F^{0.5}$	(1)
Analytical algorithms	
$Z = [2KF/(\rho L\theta)]^{0.5}$	(2)
$Z = [2/(\rho L\theta)]^{0.5}\left[86400\sum(KT_s)\right]^{0.5}$	(3)
Numerical algorithms	
$C\partial T(z,t)/\partial t = \partial[(K\partial T(z,t)/\partial z)]\partial z + I_{lat} + I_{cov}$	(4)
$I_{lat} = -L(d\theta_u/dt) = -L(\partial\theta_u/\partial T)(\partial T/\partial t)$	(5)
$C_{app} = \begin{cases} C_t & T \geq T_f \\ C_f + L(\partial\theta_u/\partial T) & T < T_f \end{cases}$	(6)
Johansen's thermal conductivity parameterization	
$K = \begin{cases} K_{dry}(K_{sat}/K_{dry})^{K_e} & \text{frozen peat} \quad (7a) \\ (K_{sat} - K_{dry})K_e + K_{dry} & \text{all other soils} \quad (7b) \end{cases}$	(7)
$K_e = \begin{cases} \theta/\theta_0 & \text{any frozen soil} & (8a) \\ (\theta/\theta_0)^2 & \text{unfrozen peat} & (8b) \\ 0.7\log(\theta/\theta_0) + 1.0 & \text{unfrozen coarse mineral soil} & (8c) \\ \log(\theta/\theta_0) + 1.0 & \text{unfrozen fine mineral soil} & (8d) \end{cases}$	(8)
$K_{sat} = \prod_{i=1}^{N}(K_i)^{\theta_i}$	(9)
$K_{dry} = \begin{cases} 0.05 & \text{unfrozen peat} & (10a) \\ 0.55 & \text{frozen peat} & (10b) \\ (0.135\rho_b + 64.7)/(2700 - 0.947\rho_b) & \text{natural mineral soil} & (10c) \\ 0.039\theta_0^{-2.2} & \text{crushed rock} & (10d) \end{cases}$	(10)
de Vries' thermal conductivity parameterization	
$K = \sum_{i=1}^{N}(f_i\theta_i K_i)/\sum_{i=1}^{N}(f_i\theta_i)$	(11)
$K = (\theta_w K_w + f_a\theta_a K_a + f_s\theta_s K_s)/(\theta_w + f_a\theta_a + f_s\theta_s)$	(12)
$f_s = \frac{1}{3}\{2/[1 + (K_s/K_w - 1)0.125] + 1/[1 + (K_s/K_w - 1)0.75]\}$	(13)
$f_a = \frac{1}{3}\{2/[1 + (K_a/K_w - 1)g_a] + [1/[1 + (K_a/K_w - 1)g_c]\}$	(14)
$g_a = \begin{cases} 0.333 - (0.333 - 0.035)\theta_a/\theta_0 & \theta_w > 0.09 \\ 0.013 + 0.944\theta_w & \theta_w \leq 0.09 \end{cases}$	(15)
$g_c = 1 - 2g_a$	(16)
Unfrozen water parameterization	
$\theta_u = a|T|^c$	(17)
$\theta_u = a|T - T_f|^c$	(18)
$\theta_u = \begin{cases} \theta_w - (\theta_w - \theta_{u,l})(T - T_f)/(T_{u,l} - T_f) & T > T_{u,l} \\ \theta_{u,l} & T \leq T_{u,l} \end{cases}$	(19)
$\theta_u = \theta_0(\psi/\psi_0)^{-1/b} = \theta_0\left[L(T - T_f)/[g(T + 273.15)\psi_0]\right]^{-1/b}$	(20)

However, applications of analytical algorithms require careful evaluation of the suitability of site conditions to algorithm assumptions [*Romanovsky and Osterkamp*, 1997], or the modification of coefficients under less favorable conditions [e.g., *Hayashi et al.*, 2007].

[8] Numerical algorithms determine the GTFD by interpolating isothermal positions from the soil temperature profile, which is numerically solved from the heat transfer equation (equation (4)). Conduction is represented in the first term of equation (4) and I_{lat} is the latent heat released or consumed during phase change of soil water and I_{cov} is convective heat transported by water flow. While I_{cov} has been cited as important in certain cases [*Hinkel and Outcalt*, 1994; *Kane et al.*, 2001], its consideration requires a fully coupled soil water model that is absent from most geothermal models [e.g., *Goodrich*, 1978; *Romanovsky et al.*, 1997; *Ling and Zhang*, 2004]. Because of the lack of available data, evaluation of models with I_{cov} exceeds the scope of this study and I_{cov} is neglected in the models tested here. Both finite difference [e.g., *Nakano and Brown*, 1972; *Goodrich*, 1978; *Verseghy*, 1991; *Foley et al.*, 1996; *Dai et al.*, 2003; *Luo et al.*, 2003; *Ling and Zhang*, 2004; *Zhang et al.*, 2003, 2007b] and finite element [e.g., *Yalamanchili and Chu*, 1973; *Goodrich*, 1982a; *Alexiades and Solomon*, 1993; *Romanovsky et al.*, 1997; *Hinzman et al.*, 1998] methods are found in numerical thermal models. However, finite element and difference equations converge to similar results for one-dimensional heat flow as long as appropriate

time and soil layer resolution is specified [*Goodrich*, 1982a; *Romanovsky et al.*, 1997; *Hinzman et al.*, 1998]. Therefore, in this study, only the more widely applied finite difference schemes are evaluated. In numerical algorithms, there are two distinct methods for the treatment of I_{lat}: (1) I_{lat} is ignored while solving equation (4) and then readjusts the soil temperature and the ratio of liquid water and ice by energy conservation during freeze and thaw [*Shoop and Bigl*, 1997; *Zhang et al.*, 2007b], and (2) I_{lat} is related to temperature and unfrozen water content (θ_u) by equation (5) and the heat capacity (C) in equation (4) is replaced by an apparent heat capacity (equation (6)) [*Nakano and Brown*, 1972; *Osterkamp*, 1987; *Hinzman et al.*, 1998; *Smirnova et al.*, 2000; *Nicolsky et al.*, 2007]. This first method, referred to here as the Decoupled Energy Conservation Parameterization (DECP), is commonly employed in LSMs [e.g., *Verseghy*, 1991; *Foley et al.*, 1996; *Dai et al.*, 2003]. The second method, referred to as the Apparent Heat Capacity Parameterization (AHCP), is often used in geothermal models. Additional reviews on numerical treatments of I_{lat} are found in *Goodrich* [1978, 1982a], *Li and Koike* [2003], and *Riseborough* [2004, pp. 300−309].

2.2. Parameterization of Soil Thermal Conductivity

[9] Thermal conductivity (K) is an important soil parameter for analytical and numerical algorithms. Among the many parameterizations [*Farouki*, 1986; *Tarnawski and Wagner*, 1992, 1993; *Riseborough*, 2004], Johansen's parameterization [*Johansen*, 1975; *Farouki*, 1986] and de Vries' parameterization [*de Vries*, 1963; *Farouki*, 1986] are most commonly found in GTFD simulations [e.g., *Verseghy*, 1991; *Tarnawski and Wagner*, 1993; *Cherkauer and Lettenmaier*, 1999; *Dai et al.*, 2003; *Zhang et al.*, 2003; *Woo et al.*, 2004; *Carey and Woo*, 2005; *Quinton et al.*, 2005; *Hayashi et al.*, 2007]. Equations (7)−(10) (referred to as complete Johansen's parameterization hereafter) summarize the variations of Johansen's parameterization under different soil conditions as reviewed by *Farouki* [1986, pp. 41−53 and 112−113]. However, only equations (7b), (8a), (9), and (10c) (referred to as commonly used Johansen's parameterization hereafter) are widely used in current LSM and hydrological applications [e.g., *Verseghy*, 1991; *Dai et al.*, 2003; *Woo et al.*, 2004; *Yi et al.*, 2006], regardless the soil condition. Equation (11) is the general form of de Vries' thermal conductivity parameterization [*de Vries*, 1963]. Although comprehensive methods to parameterize equation (11) exist [*de Vries*, 1963; *Tarnawski and Wagner*, 1992, 1993], the most commonly used parameterizations found in thermal models [e.g., *Farouki*, 1986, pp. 109−110; *Quinton et al.*, 2005; *Hayashi et al.*, 2007] are listed in equations (12)−(16).

2.3. Parameterization of Unfrozen Water Content in Frozen Soil

[10] The importance of unfrozen water content on frozen soil thermal properties and GTFD simulation has been widely demonstrated [e.g., *Anderson and Tice*, 1972; *Nakano and Brown*, 1972; *Andersland and Ladanyi*, 1994, pp. 40−43; *Osterkamp and Romanovsky*, 1997; *Romanovsky and Osterkamp*, 2000]. As soil temperature is not explicitly simulated in analytical algorithms, only a constant unfrozen water content is assigned to each type of

frozen soil [e.g., *Woo et al.*, 2004; *Carey and Woo*, 2005; *Yi et al.*, 2006], unless observations are available [e.g., *Hayashi et al.*, 2007]. Among the various relationships between unfrozen water content and subfreezing soil temperature, a power function (equation (17)) [e.g., *Anderson and Tice*, 1972; *Osterkamp and Romanovsky*, 1997; *Ling and Zhang*, 2004; *Riseborough*, 2004, p. 84; *Zhang et al.*, 2007b], a segmented linear function (equation (19)) [e.g., *Goodrich*, 1978; *Zhang et al.*, 2003; *Riseborough*, 2004, pp. 300−309] and a water potential - freezing point depression function (equation (20)) [e.g., *Cary and Mayland*, 1972; *Fuchs et al.*, 1978; *Zhao and Gray*, 1997; *Cherkauer and Lettenmaier*, 1999; *Koren et al.*, 1999; *Smirnova et al.*, 2000; *Niu and Yang*, 2006], are most commonly found in numerical algorithms. Equation (18) is a modified power function to the original form (equation (17)) [*Anderson and Tice*, 1972] by *Osterkamp and Romanovsky* [1997], in order to take into account the freezing point (T_f) depression observed in various frozen soils [*Koopmans and Miller*, 1966; *Osterkamp*, 1987; *Quinton et al.*, 2005]. Because of the empirical or semiempirical nature of the existing unfrozen water parameterization methods, site specific calibration of their empirical parameters (e.g., a, b, c, T_f, θ_u, $\theta_{u,l}$) are critical.

2.4. Boundary Conditions in GTFD Simulation

[11] The ground surface temperature (i.e., the upper boundary condition) is a key input for all GTFD algorithms. Although uncertainties in current methods to estimate [*Becker and Li*, 1995; *Klene et al.*, 2001; *Coll et al.*, 2005; *Kade et al.*, 2006] or simulate [*Verseghy*, 1991; *Hinzman et al.*, 1998; *Dai et al.*, 2003; *Zhang et al.*, 2007b] surface temperature remains one of the largest sources of error in soil thermal simulations [*Goodrich*, 1982a; *Hinzman et al.*, 1998; *Klene et al.*, 2001; *Kade et al.*, 2006], the evaluation of the methods to obtain this parameter is beyond the scope of this study. In order to reduce the uncertainty in evaluating the main algorithms and the parameterization techniques, observed soil surface (or near surface) temperatures are used as the upper boundary condition throughout this study.

[12] Certain analytical algorithms (e.g., TDSA) and all numerical algorithms require a well-defined lower boundary. Although soil temperature measured or simulated at the bottom of soil column could serve as a lower boundary condition [e.g., *Woo et al.*, 2004; *Yi et al.*, 2006], typically such inputs are unavailable. A frequently used bottom boundary conditions is a geothermal flux [e.g., *Zhang et al.*, 2003; *Ling and Zhang*, 2004; *Alexeev et al.*, 2007; *Zhang et al.*, 2007a], or zero heat flux [e.g., *Verseghy*, 1991; *Dai et al.*, 2003; *Zhang et al.*, 2007b] at a certain ground depth. However, the placement of lower boundary needs special caution [*Smerdon and Stieglitz*, 2006; *Alexeev et al.*, 2007; *Stevens et al.*, 2007], particularly when long term simulation is required.

2.5. Resolutions of Time Step and Soil Layers

[13] Changing the time step resolution in empirical and analytical algorithms results in parameter changes, yet does not affect simulation results. Changing resolution of soil layers in some analytical algorithms (e.g., TDSA and HMSA) may affect the representation of the soil physical

Table 2. Soil Profiles and Properties of the Four Sites

Site Name (Coordinates)	Depth of Soil Layers (m)	Bulk Density (kg m^{-3})	Porosity (m^3 m^{-3})	Minerals (m^3 m^{-3})	Organic (m^3 m^{-3})
Scotty Creek (SC, 61°18'N;	0.0−0.10	88.4	0.92	0.0	0.08
121°18'W, 280 m)	0.1−0.2	93.0	0.88	0.0	0.12
	0.2−0.3	134.3	0.85	0.0	0.15
	0.3−0.4	148.0	0.81	0.0	0.19
	0.4−0.5	178.5	0.77	0.0	0.23
	0.5−3.0	248.0	0.75	0.0	0.25
	>3.0	1300.0	0.43	0.57	0.0
Granger Creek (GC, 60°33'N;	0−0.03	39.8	0.94	0.0	0.06
135°11'W, 1338 m)	0.03−0.07	68.3	0.94	0.0	0.06
	0.07−0.15	80.5	0.92	0.0	0.08
	0.15−0.25	141.3	0.85	0.0	0.15
	0.25−0.35	289.8	0.75	0.05	0.20
	>0.35	1104	0.49	0.5	0.01
Wolf Creek north-facing slope	0.0−0.11	55.0	0.92	0.0	0.08
(WC_NFC, 60°31'N;	0.11−0.23	90.0	0.84	0.02	0.14
135°31'W, 1175 m)	0.23−0.60	1340.0	0.52	0.45	0.03
	>0.6	1340.0	0.52	0.47	0.01
Wolf Creek south-facing slope	0−0.4	1420.0	0.55	0.40	0.05
(WC_SFC, 60°31'N;	>0.4	1420.0	0.55	0.43	0.02
135°31'W, 1175 m)					

properties in vertically heterogeneous soils (e.g., ρ, K, and θ), influencing GTFD simulations. However, the resolutions of the time step and soil layers are critical in all the numerical thermal models, due mainly to their influence on the converging behavior in solving equation (4) [*Lunardini*, 1981, p. 473; *Goodrich*, 1982a]. Coarse simulations may create oscillations in simulation results of soil temperature and GTFD or even failures of model runs. Theoretically, the finer the time resolution with a greater number of thinner soil layers, the more accurate the soil temperature and GTFD simulation. Very often, a finer resolution in time requires more and thinner layers in the soil. However, finer resolution dictates increased input requirements, computing resources and parameterizations. In practice, determining the resolution of time steps and soil layers is also affected by the time and spatial scales of application. A balance must be achieved between simulation accuracy and computational efficiency.

3. Study Sites and Methodology
3.1. Sites and Field Measurements

[14] All four model testing sites are located in Canada's discontinuous permafrost regions above 60°N latitude. Scotty Creek (referred to as SC hereafter) is located in a wetland-dominated region near Fort Simpson, Northwest Territories. The three other sites are located within the Wolf Creek Research Basin, Yukon Territory. Granger Creek (a subcatchment of Wolf Creek, and referred to as GC hereafter) is located on a north-facing slope above tree line. Two sites located across a river valley are referred to as the north-facing slope (WC_NFS hereafter) and south-facing slope (WC_SFS hereafter). Additional details and site descriptions can be found in *Carey and Woo* [2001, 2005], *Quinton et al.* [2005], and *Hayashi et al.* [2007]. Table 2 summarizes observed soil properties required for model parameterization. Except for WC_SFS which has only mineral soils, the sites have 0.2−3.0 m of organic soils at the surface which are subdivided into layers with increasing bulk density and porosity with depth. Both SC and GC are underlain with permafrost, whereas no permafrost

was observed at WC_NFS and WC_SFS during the study periods.

[15] At WC_NFS and WC_SFS, ground temperatures were measured using type-T thermocouples and liquid soil water content using site-calibrated TDR (MoisturePoint) probes. At GC and SC, soil temperature was measured using thermistors and liquid water content was measured using site-calibrated Campbell Scientific water content reflectometers (CS-615). Instrumentation details and the site calibration of probes can be found in *Carey and Woo* [1998, 2001, 2005] for WC_NFS and WC_SFS and in *Quinton et al.* [2005] and *Hayashi et al.* [2007] for GC and SC. Table 3 provides data periods, depths of observation and selected annual averaged variables for the sites. All sites covered two thawing and freezing seasons with the exception of WC_SFS which covered two thawing and one freezing season. At SC, GC, and WC_NFS, the first thawing and freezing seasons were considered for model calibration to derive parameters such as β for equation (1) and unfrozen water parameters for equations (18)−(20). The second thawing and freezing season were used for model evaluation. At WC_SFS, the first thawing season served as model calibration and the second for evaluation, while the one freezing season was used for both purposes. While soil moisture data at WC_NFS and WC_SFS were absent during winter months (October to March), all other observations continued through the data periods in Table 3, with occasional missing values.

3.2. Algorithms to be Evaluated and Their Coding Techniques

[16] Five GTFD algorithms from three categories were selected for comparison in this study. Their input and parameter requirements, outputs and references are provided in Table 4. The semiempirical ATIA has the least input parameter requirements, yet the empirical coefficient β must be obtained with sufficient observations of GTFD at individual sites. The four analytical and numerical algorithms do not require *in situ* observed GTFD for model calibration, yet require more inputs and soil parameters. Furthermore,

Table 3. Data Periods, Observation Depths, and Annual Average Values of Soil Temperature and Moisture

Site	Data Periods	Soil Temperature Observation Depth (m)	$T_{s,\,ann}/T_{b,ann}$ (°C)	Soil Water Observation Depth (m)	θ_{ann} at Each Layer (m³ m⁻³)
SC	1 September 2003 – 31 August 2005	0, 0.05, 0.1, 0.15, 0.2, 0.25, 0.3, 0.4, 0.5, 0.6, 0.7	3.2/0.3	0.1, 0.2, 0.3, 0.4	0.42,0.54,0.65, 0.64
GC	20 July 2001 – 24 August 2003	0.02, 0.05, 0.075, 0.1, 0.15, 0.2, 0.25, 0.3, 0.35, 0.4	−0.2/−0.9	0.02, 0.05, 0.1, 0.2, 0.3, 0.4	0.18,0.18,0.17, 0.20,0.35,0.41
WC_NFS	10 April 1996 – 22 April 1998	0.02, 0.05, 0.2, 0.4, 0.6, 1.0, 1.2, 1.4	2.1/0.9	0.05, 0.1, 0.2, 0.4, 0.6	0.37,0.46,0.39, 0.43,0.38
WC_SFS	12 April 1996 – 22 September 1997	0.02, 0.05, 0.2, 0.4, 0.6, 1.0, 1.5	0.4/1.3	0.05, 0.1, 0.2, 0.4, 0.6, 1.0	0.20,0.22,0.22, 0.25,0.24,0.16

soil specific calibration for unfrozen water parameterization is critical to analytical and numerical algorithms. The primary difference between the two analytical algorithms are: (1) TDSA operates with both surface and bottom forcing while HMSA only requires surface forcing, and (2) TDSA quantifies the thawing and freezing penetration layer by layer, allowing identification of multiple GTFD, whereas HMSA can only calculate the top first thawing or frozen front. Both numerical methods, FD_DECP and FD_AHCP, use finite difference numerical schemes to discretize equation (4) and are identical except for the treatment of I_{lat}. FD_DECP employs the decoupled energy conservation method and FD_AHCP uses the apparent heat capacity method described above. ATIA, HMSA, FD_DECP, and FD_AHCP were coded in C++ while TDSA remained in FORTRAN90 as supplied by the developers [*Woo et al.*, 2004].

[17] Three soil thermal conductivity parameterizations: (1) the complete Johansen's parameterization (equations (7)–(10)), (2) the commonly used Johansen's parameterization (equations (7b), (8a), (9), and (10c)), and (3) de Vries' parameterization (equations (12)–(16)), were added to all algorithms except ATIA. Three unfrozen water parameterizations: (1) power function (equation (18)), (2) segmented linear function (equation (19)), and (3) water potential-freezing point depression function (equation (20)), were added to FD_DECP and FD_AHCP. A constant unfrozen water content ($\theta_{u,l}$) under subfreezing conditions was assigned to each soil type for HMSA and TDSA. All algorithms were coded to allow soil layers and node spacing, time step, boundary conditions and placement of the lower boundary to be easily adjusted and tested.

3.3. Preparation of Model Inputs, Parameters, and Evaluation Data

[18] Continuous inputs of soil temperature at the top and bottom boundary and the total and liquid water content for all soil layers are required during both calibration and evaluation periods. Total moisture content during frozen periods was taken as a constant and estimated from the observed moisture content prior to freezing. Liquid water contents during winter at WC_NFS and WC_SFS were estimated based on the subfreezing temperature–unfrozen water content relation from observed data. Missing data was gap-filled by interpolation or extrapolation of the known values. Soil moisture content at soil layers other than observation depth was determined either by interpolation or calibrated using data during model calibration period (details in section 3.4).

[19] Parameters for the unfrozen water–subfreezing temperature relationships (equations (18)–(20)) were obtained from observations at the four sites. Figure 1 shows the observed unfrozen water content under subfreezing temperature for two selected soil layers at the four sites, and the fit curves by the three unfrozen parameterization methods. Parameters T_f, $T_{u,l}$ and $\theta_{u,l}$ are determined by the inflection points and the minimum unfrozen water content observed. Because of the limited sample size and narrow soil temperature range, mathematical methods of curve fitting failed to determine values of a, b, and c in equations (18) and (20). Alternatively, these coefficients were manually determined by trial and error methods to best fit the observed curves, and a complete set of unfrozen water parameters derived from the first thawing and freezing season are listed in Table 5. The observed freezing point (T_f) ranged from −0.3 to 0°C,

Table 4. Summary of the Five GTFD Simulation Algorithms

| Algorithm	Category	Driving Variables	Parameters	Outputs	References
ATIA	semiempirical	T_s	β	single GTFD	*Nelson and Outcalt* [1987], *Hinkel and Nicholas* [1995]
HMSA	analytical	T_s	z, θ_0, ρ_b, θ_i ($i = 1, N$) for each soil layer	single GTFD	*Hayashi et al.* [2007]
TDSA	analytical	T_s and T_b	same as HMSA	multiple GTFD	*Woo et al.* [2004], *Yi et al.* [2006]
FD_DECP	numerical	(a) T_s or Hf_s; (b) T_b or Hf_b	(a) z, θ_0, ρ_b, θ_i ($i = 1,N$) for each soil layer; (b) empirical parameters for equation (18) or equation (19) or equation (20) for each soil layer	(a) $T(z, t)$ for each soil layer and (b) multiple GTFD	*Verseghy* [1991], *Foley et al.* [1996], *Shoop and Bigl* [1997], *Dai et al.* [2003], *Zhang et al.* [2003, 2007b]
FD_AHCP	numerical	same as FD_DECP	same as FD_DECP	same as FD_DECP	*Nakano and Brown* [1972], *Goodrich* [1978], *Smirnova et al.* [2000], *Nicolsky et al.* [2007]
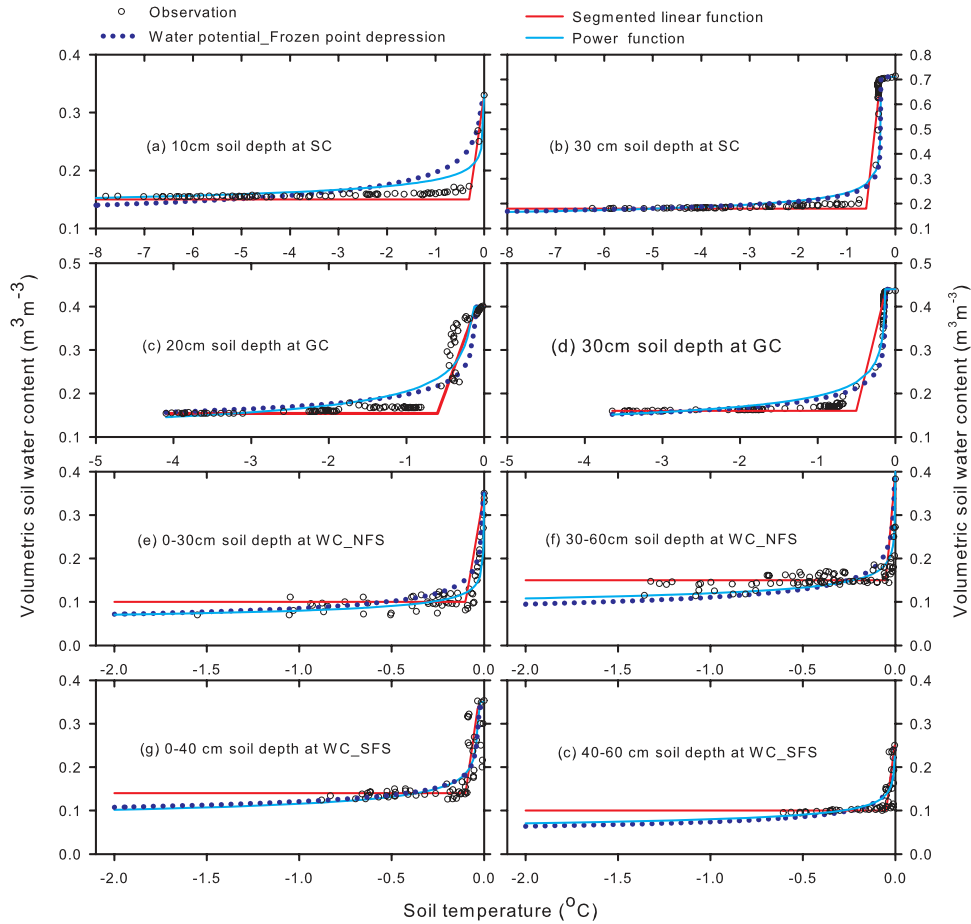
Figure 1. Comparisons of observed and simulated unfrozen water content under subfreezing soil temperature using three unfrozen water parameterizations at two soil layers for the four model testing sites.

with more depression in organic soils below 0.1–0.2 m soil depth.

[20] Because of the freezing point depression, the conventional 0°C isothermal position does not represent GTFD at the study sites. Alternatively, observed T_f values for each soil layer listed in Table 5 were used to determine observed and simulated GTFD from the soil temperature profile. Gap-filled data was not used in the evaluation of GTFD. For node spacing of soil temperature measurement greater than 0.2 m, linear interpolation of T_f position may cause substantive errors due to the nonlinear soil temperature

profile and frequently observed zero-curtain effect [*Outcalt et al.*, 1990; *Hinkel and Outcalt*, 1994; *Osterkamp and Romanovsky*, 1997], and values interpolated more than 0.1 m from the sensor position were discarded. The same 0.1 m rule was applied when evaluating temperature profiles simulated with FD_DECP and FD_AHCP. Multiple thawing and freezing fronts can be identified in observed data and by several GTFD algorithms (Table 4), yet only the top thawing and freezing fronts were analyzed in this study to avoid unnecessary complexity. Observed GTFD values were used to determine β values required by ATIA (equation (1))

Table 5. Values for the Three Unfrozen Water Parameterizations at the Four Sites

Site	Soil Layer (m)	Soil Texture	T_f	$T_{u,l}$	$\theta_{u,l}$	a	c	b
SC	0–0.1	surface organic	0.0	−0.3	0.15	0.184	−0.09	6.2
	0.1–0.2	peat	−0.05	−0.3	0.18	0.22	−0.15	6.7
	0.2–0.3	peat	−0.3	−0.6	0.18	0.23	−0.16	7.1
	>0.4	peat	−0.05	−0.3	0.18	0.22	−0.15	6.7
GC	0–0.1	surface organic	−0.05	−0.2	0.13	0.14	−0.05	5.2
	0.1–0.2	peat	−0.1	−0.6	0.15	0.2	−0.23	6.4
	0.2–0.35	peat	−0.12	−0.5	0.16	0.19	−0.18	6.7
	>0.35	sandy loam	−0.12	−0.3	0.18	0.18	−0.1	9.5
WC_NFS	0–0.3	surface organic	0	−0.1	0.1	0.08	−0.18	4.0
	>0.3	silt	0	−0.05	0.15	0.12	−0.15	4.5
WC_SFS	0.–0.4	silt	−0.03	−0.1	0.14	0.115	−0.18	6.2
	>0.4	silt	0	−0.05	0.1	0.08	−0.18	4.7

Table 6. β Values at the Four Testing Sites During Two Thawing/Freezing Seasons

Site	SC		GC		WC_NFS		WC_SFS	
Season	2003–2004	2004–2005	2001–2002	2002–2003	1996–1997	1997–1998	1996–1997	1997–1998
β for freezing	0.067	0.046	0.070	0.102	0.089	0.067	0.061	...
β for thawing	0.023	0.025	0.023	0.021	0.045	0.053	0.068	0.083

from regressions between GTFD and the F values calculated from surface temperature. Although Table 6 lists all β values at all sites for both thawing and freezing over two seasons, only values from the first season were used in algorithm evaluation to test its interannual transferability.

3.4. Evaluation Strategy

[21] GTFD simulations are influenced by the algorithms used, soil thermal parameterization and model configuration. In addition, the prescription method (outlined as Runs 1–3 in Table 7) is critical in cases where data are unavailable, which is common in permafrost environments. Run1 is supplied with the best available inputs at the sites. The simulated soil column depth in Run1is confined in the soil column with known soil boundary temperature at the top and bottom. Where soil surface temperature is not measured, the top available soil temperature (at 0.02 m) is used as the upper boundary condition. The total (water and ice) and liquid soil moisture contents are supplied for all the simulated soil layers. Run2 represents a condition when the lower boundary condition is unknown, but a zero heat flux is assumed at 5-m depth. Total and liquid soil moisture contents below the observation depths were calibrated using the first year's data such that the RMSD between the simulated and observed GTFD is minimized. Run3 represents a condition when the soil moisture and lower boundary are unknown, which is typically the case for spatial modeling in permafrost regions. Because of the large

snowmelt water supply during soil thawing [Woo, 1986; McNamara et al., 1998; Carey and Woo, 1998], the simplest and most physically reasonable assumption is a saturated soil condition. Run3 is designed to test the efficacy of such a simple assumption in various permafrost sites. While tests of all possible permutations in model algorithms, parameterizations and data prescriptions are infeasible, it is possible to reasonably evaluate one experimental variable at a time by careful experimental design.

[22] Model configurations such as time step, soil layer resolution, and placement of the lower boundary condition, are largely related to the application and spatial time scales [Smerdon and Stieglitz, 2006; Alexeev et al., 2007; Nicolsky et al., 2007; Zhang et al., 2007b], yet a thorough evaluation of those settings exceed the scope of this study. The following iterative procedure was followed to ensure the chosen model configuration would not disturb algorithm and parameterization evaluations made in this study. To obtain the optimal time resolution for the two numerical algorithms, an estimated "good" soil layer resolution and column depth was used for different time resolution runs at the four sites. The Root Mean Squared Differences (RMSD) of simulated GTFD between runs with different time resolutions were compared to an arbitrary threshold value of 0.01 m, which is considerably smaller than observation GTFD errors (<0.05 m in upper and <0.1 m in lower layers). Once the RMSD was smaller than 0.01 m, the desired time resolution was reached. Following this, the optimal time

Table 7. Model Inputs and Configurations for the Three Sets of Model Runs

| Inputs and Configurations	Run1	Run2	Run3
Bottom of soil column	0.7 m at SC; 0.4 m at GC; 1.4 m at WC_NFS; 1.5 m at WC_SFS	5 m	5 m
Soil layers and node spacing, m	SC (8): 0.05, 0.05, 0.1, 0.1, 0.1, 0.1, 0.1, 0.1 GC (8): 0.03, 0.05, 0.05, 0.05, 0.05, 0.05, 0.05, 0.05; WC_NFS (13): 0.04, 0.05, 0.06, 0.06, 0.07, 0.1, 0.1, 0.1, 0.1, 0.1, 0.2, 0.2, 0.2; WC_SFS (13): 0.03, 0.05, 0.1, 0.1, 0.1, 0.1, 0.1, 0.1, 0.1, 0.1, 0.2, 0.2,0.2	All sites (16): 0.05, 0.05, 0.1, 0.1, 0.1, 0.1, 0.1, 0.1, 0.1, 0.2, 0.4, 0.6, 0.6, 0.6, 0.8, 1.0	same as in Run2
Computing time step	1 day for ATIA, HMSA and TDSA; 30 min for FD_DECP and FD_AHCP	same as in Run1	same as in Run1
Top boundary condition	observed surface or near surface soil temperatures	same as in Run1	same as in Run1
Bottom boundary condition	observed bottom soil temperatures	HMSA and TDSA: not applicable. FD_DECP and FD_AHCP: $Hf_b = 0$	same as in Run2
Soil moisture content	observed or estimated	observed for known soil layers and estimated/calibrated for other layers	saturation for all layers at all time
Unfrozen water content	observed or estimated	observed for known soil layers and estimated/calibrated for other layers	determined by equation (18) at SC site and by equation (19) at other sites
K parametrization	de Vries'	de Vries'	de Vries'
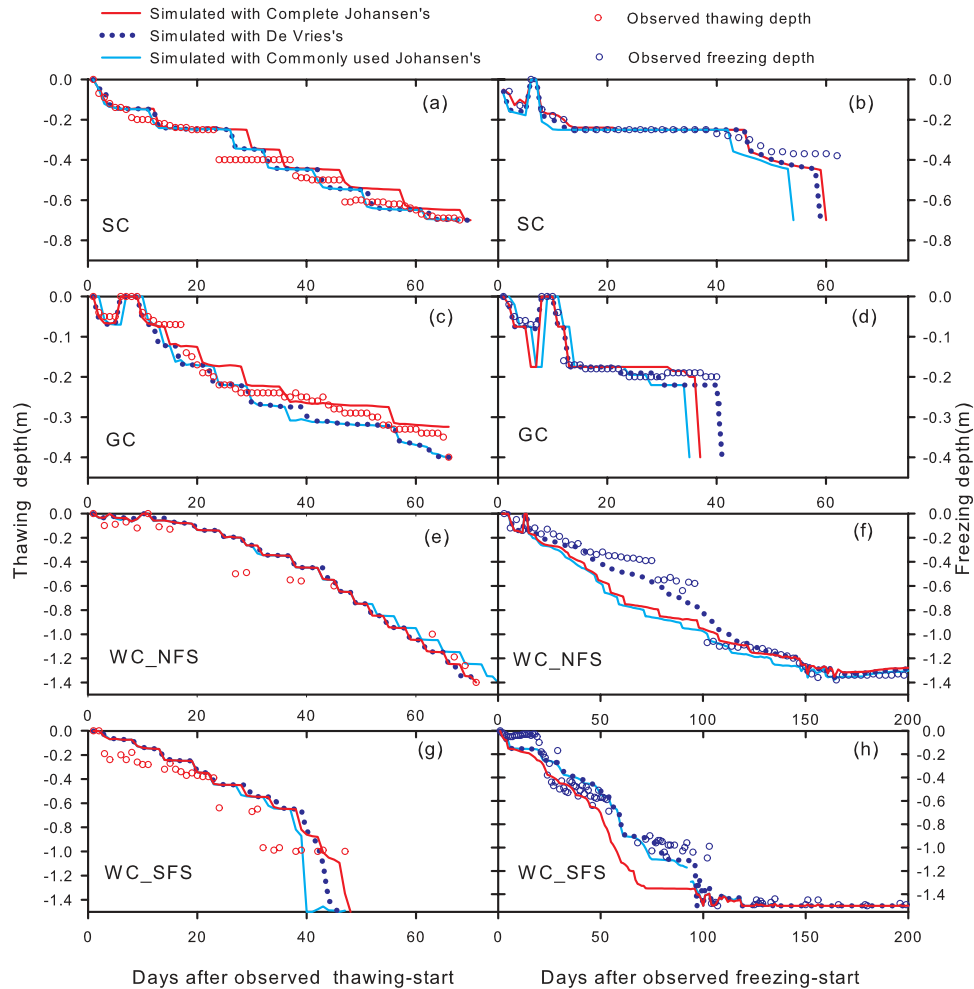
Figure 2. Comparisons of observed and simulated ground thawing (left) and freezing (right) depths by FD_AHCP at the four testing sites with three different soil thermal conductivity parameterizations.

resolution was applied to evaluate soil layer resolution and the zero heat flux position. Node spacing requires thinner layers in the active layer and layers progressively thicken with depth. After the optimal configurations were found utilizing the same 0.01-m criteria, this node spacing was reapplied to runs for time resolution testing and repeated until all the best settings became stable. A 30-minute time resolution, 16-layer soil resolution (as for Run2 in Table 7), and a 5-m-deep soil column were found to be adequate for FD_DECP and FD_AHCP at the four testing sites during the one year model evaluation period.

[23] Comparison of the three soil thermal conductivity parameterizations and the three unfrozen water parameterizations were performed by Run1 (Table 7), which supplied the best possible inputs. Evaluation was performed by comparing simulated GTFD with observed values at each site. The thermal conductivity parameterizations were evaluated first using observed unfrozen water content. The best thermal conductivity parameterization method was then used in the runs to evaluate the unfrozen water parameterizations by substituting the observed unfrozen water with calculated values.

[24] Once the best possible model configurations and soil parameterizations were found, they were applied to each of the four algorithms (not applicable for ATIA) to simulate the GTFD at the four sites during the model evaluation periods with the three sets of run conditions as listed in Table 7. The RMSD between the simulated and observed values were then calculated to evaluate the five algorithms.

4. Results

[25] Evaluations of soil parameterizations and algorithms for GTFD simulation are presented in Figures 2–7 and Tables 8–10. As the three soil thermal conductivity and unfrozen water parameterizations showed variation in results among the sites, not among the algorithms for a site, only results from the FD_AHCP model will be discussed for clarity. In order to keep the same sample size for comparison, the RMSD analysis only considers the top thawing or freezing front.

4.1. Observed Thawing/Freezing Features at the Four Sites During Evaluation Periods

[26] At SC from 1 September 2004 to 31 August 2005, subfreezing soil surface temperature lasted 200 days and thawing surface temperature lasted 165 days (Figure 4a). Soil surface temperature ranged from a maximum of 24.4°C
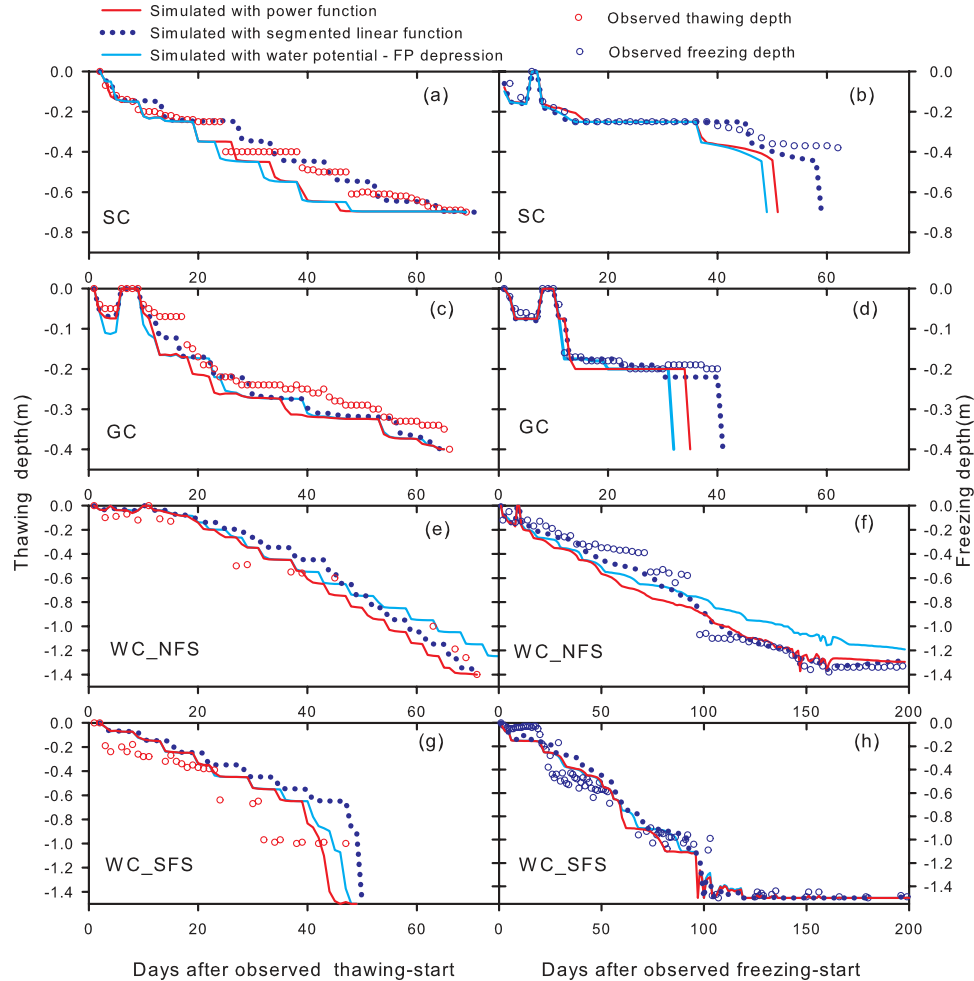
Figure 3. Comparison of observed and simulated ground thawing (left) and freezing (right) depths by FD_AHCP at the four testing sites with three different unfrozen water parameterizations.

to a minimum of −5.7°C. During the first 62 days of freezing, the upper freezing front progressed slowly to 0.4 m, halting at several depths (Figures 2b and 4) due to the zero-curtain effect above the freezing front. The upper and lower freezing fronts merged at day 62 of freezing, closing the active layer, a typical feature at permafrost sites [*Hinkel and Outcalt*, 1994; *Osterkamp and Romanovsky*, 1997]. Thawing proceeded 68 days until passing the lowest sensor and the temperature at 0.7 m indicated that thawing continued to progress (Figure 4a). The maximum Active Layer Thickness (ALT) found by FD_AHCP simulation (Run2) was 1 m.

[27] At GC from 25 August 2002 to 24 August 2003, subfreezing temperature at 0.02 m lasted 240 days and thawing 125 days, with maximum and minimum temperatures of 11.5°C and −15.8°C respectively (Figure 5a). After 40 days of freezing, the upper and lower fronts met at 0.2 m, closing the active layer (Figures 2d and 5). Thawing proceeded 66 days until passing the lowest sensor position, halting occasionally at certain depths (Figure 2a). Thawing proceeded after passing the lowest sensor at 0.4 m, and maximum ALT from FD_AHCP (Run2) is approximately 0.6 m.

[28] At WC_NFS from 20 April 1997 to 19 April 1998, subfreezing temperatures at 0.02 m lasted 203 days, thawing temperatures 163 days, and annual maximum and minimum temperatures were 20.5°C and −4.2°C (Figure 6a). Thawing proceeded for 70 days until the lowest sensor at 1.4 m was passed (Figure 2a). The soil freezing front proceeded slowly, and after 150 days reached its greatest depth of 1.35 m. No near-surface permafrost was found during the model evaluation for WC_NFS (Figures 2f and 6).

[29] For WC_SFS between 20 September 1996 and 19 September 1997, subfreezing temperatures at 0.02 m lasted 218 days, thawing temperatures 147 days, and maximum and minimum temperatures were 12.5°C and −10.5°C (Figure 7a). After 103 days, the freezing front reached a maximum depth of 1.48 m. After 47 thawing days, the profile became frost-free as the upper and lower thawing front met at 1.0 m depth (Figures 2g and 7). No near-surface permafrost was observed during model evaluation for WC_SFS.

4.2. Evaluation of Soil Thermal Conductivity Parameterizations

[30] Although the simulated GTFD with the three methods followed the observations (Figure 2), the RMSD (Table 8)
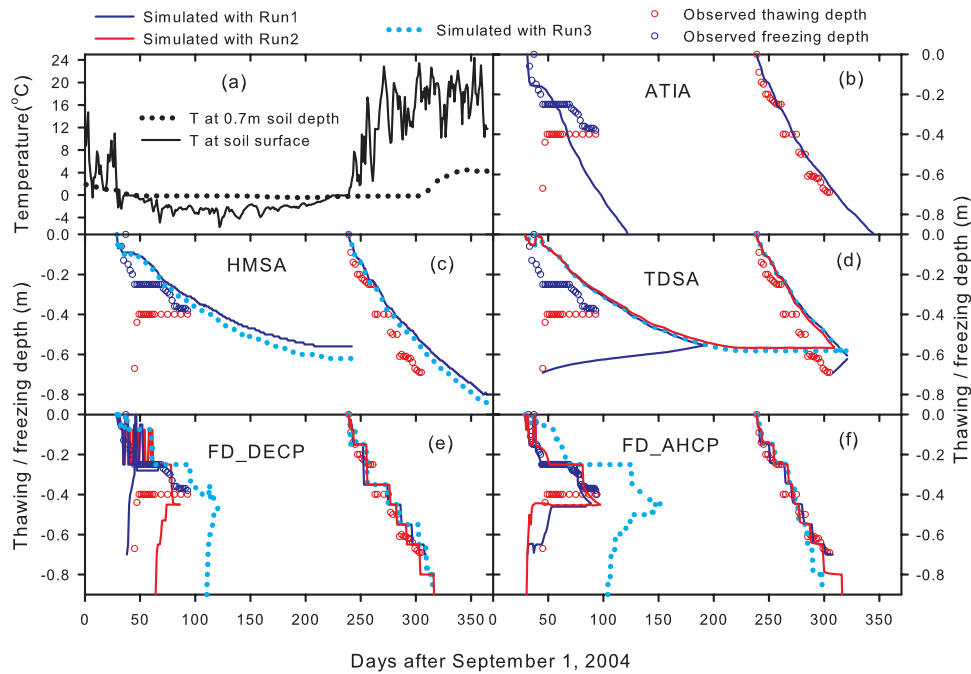
Figure 4. (a) Observed surface and bottom temperatures during the evaluation period. (b)−(f) Comparisons of observed and simulated thawing and freezing depths at Scotty Greek with five algorithms and three sets of model runs.

revealed that the De Vries' *parameterization* performed best at all sites except the thawing simulation at WC_SFS where the complete Johansen's parameterization performed slightly better (Figure 2g). Aside from the freezing simulation at WC_SFS (Figure 2h), the complete Johansen's parameterization performed similarly or better than the commonly used Johansen's parameterization for both freezing and thawing. Discrepancies of simulated GTFD by the three parameterizations were smaller at the beginning of freezing and thawing compared with their later stages. The largest discrepancies occurred in the later freezing stages of the permafrost sites (Figures 2b and 2c) and in later thawing
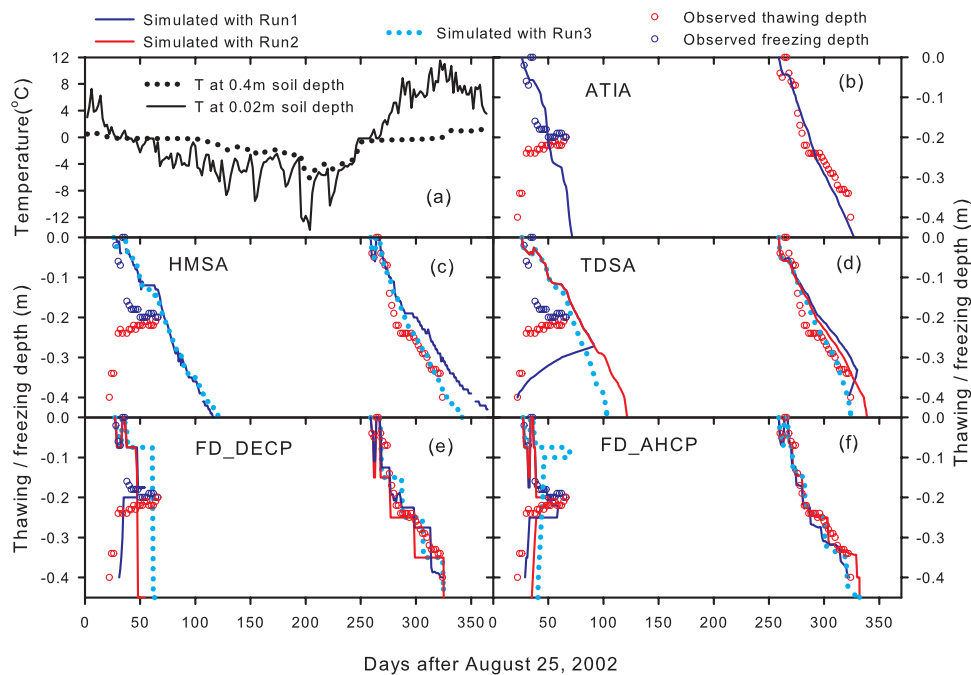

Figure 5. (a) Observed surface and bottom temperatures during the evaluation period. (b)−(f) Comparisons of observed and simulated thawing and freezing depths at Granger Greek with five algorithms and three sets of model runs.
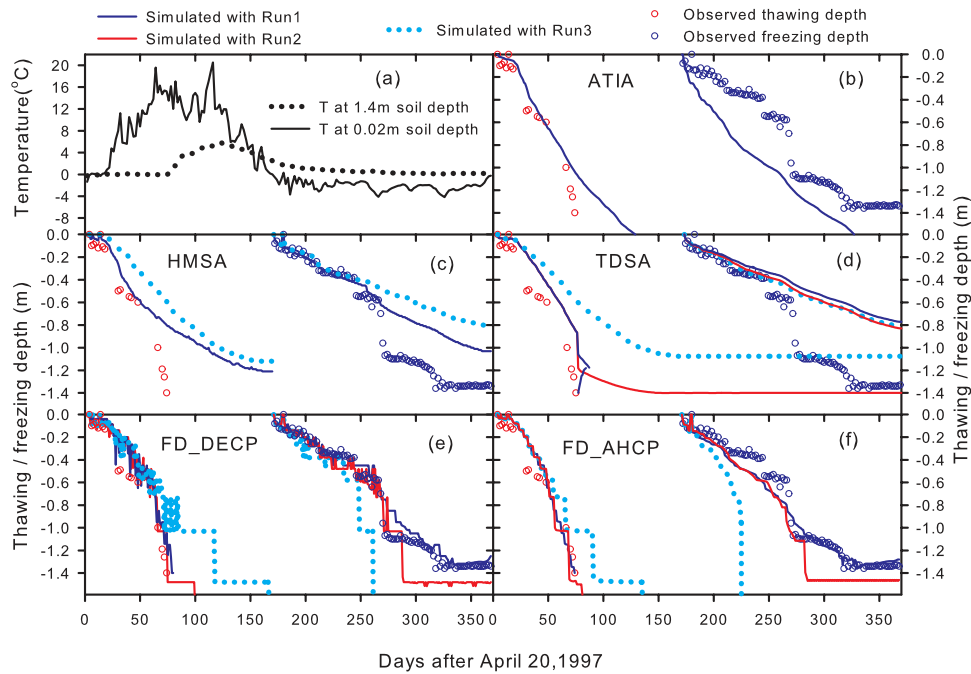
Figure 6. (a) Observed surface and bottom temperatures during the evaluation period. (b)−(f) Comparisons of observed and simulated thawing and freezing depths at a north-facing slope in Wolf Creek with five algorithms and three sets of model runs.

stage of the WC_SFS site (Figure 2g), when the two freezing or thawing fronts merge.

4.3. Evaluation of Unfrozen Water Parameterizations

[31] The large number of unfrozen water content observations at multiple soil depths and subfreezing temperatures

for SC and GC (Figures 1a, 1b, 1c, 1d) enabled the determination of unfrozen soil parameters (Table 5). At WC_SFS and WC_NFS, soil water measurements were absent during most of the freezing periods, and unfrozen water−soil temperature observations were only available from 0 to −1°C (Figures 1e, 1f, 1g, 1h). Although similar
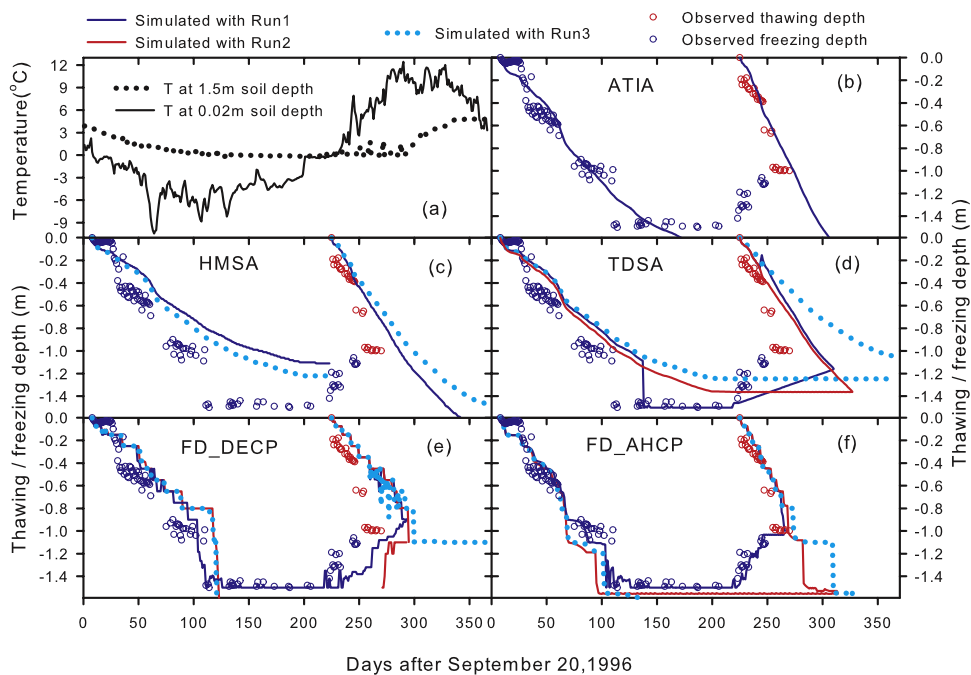

Figure 7. (a) Observed surface and bottom temperatures during the evaluation period. (b)−(f) Comparisons of observed and simulated thawing and freezing depths at a south-facing slope in Wolf Creek with five algorithms and three sets of model runs.

Table 8. The RMSD (m) Between Observed and Simulated GTFD by FD_AHCP With Three Soil Thermal Conductivity Parameterizations at the Four Sites

Process	Methods	SC	GC	WC_NFS	WC_SFS
Thawing depth	complete Johansen's	0.05	0.03	0.17	0.16
	commonly used Johansen's	0.05	0.04	0.20	0.19
	de Vries'	0.05	0.03	0.08	0.18
Freezing depth	complete Johansen's	0.08	0.09	0.10	0.19
	commonly used Johansen's	0.13	0.09	0.10	0.12
	de Vries'	0.08	0.05	0.10	0.10

curves to SC and GC were obtained, their parameters were less reliable, particularly with regards to the predictions beyond the observed subfreezing soil temperature range ($<-1.0°C$). With carefully selected parameters, all three methods followed the same trend of observed unfrozen water variation with subfreezing soil temperature (Figure 1). However, discrepancies occurred in certain temperature ranges. For example, the segmented linear function provided a better fit to the observations at 0.1-m soil depth at SC (Figure 1a), while the other methods gave a better prediction at 0.3 m for GC. GTFD simulated with the three unfrozen water parameterization methods followed similar trends as observations, yet discrepancies did exist in certain periods at several sites (Figure 3). RMSD analysis (Table 9) indicated that the segmented linear function performed better than or the same as the other two methods at the three sites with organic cover (SC, GC and WC_NFS), but not at the mineral soil site (WF_SCS). The other two unfrozen soil parameterization methods exhibited little difference among all sites. The discrepancy in simulated GTFD among the three unfrozen water parameterizations increase as thawing/freezing proceeded to deeper depths (Figure 3), indicating the cumulative effect of their differences.

4.4. Evaluation of the Semiempirical Algorithm ATIA

[32] ATIA is the simplest algorithm with only one model parameter (β) and one input variable (T_s). Regardless, ATIA provided reasonable estimates of thaw depths at the two permafrost sites even when β values were determined from other seasons (Figures 4b and 5b). Furthermore, ATIA (along with FD_AHCP) produced the best simulations of freezing depth at the seasonal frost site WC_SFS, although the β value used for prediction was derived from the same data set (Table 10 and Figure 7b). When thawing (at seasonal frost sites) and freezing (at permafrost sites) processes were affected by bottom forcing, ATIA performed badly, particularly in the later thawing/freezing stages. The large error in the simulation of freezing depth by ATIA at WC_NFS (Figure 6b) was caused by the interannual variation in β (Table 6). The thawing β values calibrated with

GTFD observations at the four sites ranged from 0.023 to 0.083, while freezing β values ranged from 0.046 to 0.102. The interannual variation of β ranged from 8% to 37% over the two seasons.

4.5. Evaluation of the Analytical Algorithms HMSA and TDSA

[33] Unlike ATIA, the two analytical algorithms do not require *in situ* observations of GTFD to calibrate model parameters. However, they require inputs of soil thermal conductivity (K), or other soil physical variables (Table 4) to derive K. Normally, these parameters are basic inputs or simulated variables in most LSMs and hydrological models [e.g., *Verseghy*, 1991; *Cherkauer and Lettenmaier*, 1999; *Dai et al.*, 2003; *Niu and Yang*, 2006]. While HMSA only requires T_s as an input, TDSA requires soil temperature at the soil bottom when its two-directional function is enabled (Run1). Unfrozen water content can be parameterized in analytical algorithms, yet only with a constant value for each soil type ($\theta_{u,i}$). The RMSD analysis (Table 10) indicates that simulation of GTFD by HMSA and TDSA were worse than the semiempirical ATIA at most sites with the exception of freezing depths at SC and thawing depths at WC_SFS. When the two-directional function is disabled (Run2), TDSA performs similar to HMSA at almost all sites (c and d in Figures 4−7). With the bottom boundary condition included, TDSA (Run1) did improve GTFD simulations at all sites (d in Figures 4−7), but those improvements were not reflected in Table 10 as the second thawing/freezing fronts were excluded in RMSD analysis. Assuming soil saturation (Run3) caused little difference in the two permafrost sites, yet large errors occurred at the two seasonally frozen sites. Figures 4−7 (c and d) indicate that both analytical algorithms underestimate GTFD, particularly at later thawing/freezing stages.

4.6. Evaluation of the Numerical Algorithms FD_DECP and FD_AHCP

[34] The additional parameters required by numerical models compared to analytical algorithms (Table 5) allow

Table 9. The RMSD (m) Between Observed and Simulated GTFD by FD_AHCP With Three Unfrozen Water Parameterizations at the Four Test Sites

Process	Methods	SC	GC	WC_NFS	WC_SFS
Thawing depth	power function	0.08	0.05	0.12	0.1
	water potential−freezing point depression function	0.09	0.05	0.10	0.1
	segmented linear function	0.05	0.03	0.10	0.12
Freezing depth	power function	0.15	0.04	0.15	0.18
	water potential−freezing point depression function	0.16	0.04	0.18	0.18
	segmented linear function	0.09	0.04	0.08	0.23

Table 10. The RMSD (m) of GTFD Between the Observations and Simulations by the Five Algorithms With Three Run Scenarios at the Four Testing Sites During the Evaluation Periods

	RMSD for Thaw Depth, m			RMSD for Frozen Depth, m		
	Run1	Run2	Run3	Run1	Run2	Run3
Scotty Creek						
ATIA	0.05	. . .	. . .	0.13	. . .	. . .
HMSA	0.11	. . .	0.10	0.09	. . .	0.08
TDSA	0.14	0.12	0.13	0.12	0.13	0.13
FD_DECP	0.07	0.06	0.07	0.18	0.13	0.11
FD_AHCP	0.05	0.07	0.16	0.03	0.04	0.11
Granger Creek						
ATIA	0.04	. . .	. . .	0.09	. . .	. . .
HMSA	0.05	. . .	0.03	0.17	. . .	0.17
TDSA	0.06	0.04	0.04	0.18	0.18	0.17
FD_DECP	0.04	0.05	0.04	0.09	0.09	0.18
FD_AHCP	0.03	0.02	0.03	0.05	0.07	0.16
Wolf Creek, north-facing slope						
ATIA	0.15	. . .	. . .	0.13	. . .	. . .
HMSA	0.30	. . .	0.37	0.19	. . .	0.28
TDSA	0.24	0.24	0.37	0.30	0.28	0.28
FD_DECP	0.16	0.16	0.27	0.04	0.12	0.13
FD_AHCP	0.10	0.11	0.15	0.02	0.13	0.13
Wolf Creek, south-facing slope						
ATIA	0.19	. . .	. . .	0.10	. . .	. . .
HMSA	0.17	. . .	0.21	0.31	. . .	0.26
TDSA	0.20	0.25	0.51	0.20	0.22	0.26
FD_DECP	0.25	0.30	0.48	0.16	0.22	0.22
FD_AHCP	0.17	0.22	0.24	0.10	0.16	0.18

Note· · ·: The designated run is not applicable.

detailed soil thermal properties (C and K), and the freezing point depression (T_f), a critical parameter for soil thawing and freezing simulation in permafrost soils [*Osterkamp*, 1987; *Osterkamp and Romanovsky*, 1997; *Torrance and Schellekens*, 2006], to be properly considered. The FD_AHCP with best inputs (Run1) provided the best simulations of GTFD among all the algorithms for all the thawing and freezing processes at the four sites (Figures 4–7 and Table 10). With a zero heat flux assumption at 5-m soil depth (Run2), FD_AHCP still performed better or comparable with the other algorithms at all sites except WC_SFS. When soil saturation was assumed (Run3), the results simulated by FD_AHCP were only marginally better than the empirical and analytical algorithms. The performance of FD_DECP was similar to FD_AHCP in most cases, yet its treatment of latent heat during thawing/freezing resulted in more abrupt changes and oscillations in the simulated GTFD (Figures 4e, 6e, and 7e), resulting in occasionally large RMSD (Table 10), particularly when less favorable inputs were supplied (Run2 and Run3).

5. Discussion and Conclusions

[35] With detailed filed observations and carefully designed model configurations, five GTFD simulation algorithms, three soil thermal conductivity parameterizations and three unfrozen water parameterization methods were evaluated for soil with both seasonal frost and permafrost. The following recommendations are made to improve the simulations of soil thawing and freezing processes in current land surface modeling, hydrological modeling and geothermal modeling in permafrost regions.

[36] (1) de Vries' parameterization (equations (12)–(16)) are recommended as the best method to parameterize the thermal conductivity in permafrost soils. It achieved improved results from the commonly used Johansen's parameterization (equations (7b), (8a), (9), and (10c)) in both thawing and freezing simulations at all sites. Some modifications of Johansen's parameterization under a frozen condition and different soil types (equations (7), (8), and (10)) improved the GTFD simulation at the three sites with organic cover, but not the freezing simulation at the mineral soil site (WC_SFS), indicating improvements of their parameters under such conditions is needed.

[37] (2) The three unfrozen water parameterizations with carefully chosen coefficients exhibited little difference in terms of GTFD simulations, although the segmented linear function (equation (19)) performed slightly better at the three sites with organic soils (SC, GC and WC_NFS) while the other two methods (equations (18) and (20)) performed slightly better at the mineral soil site (WC_SFS). Since all the three parameters (T_f, $T_{u,l}$, and $\theta_{u,l}$) of the segmented linear function have physical meaning, it is the easiest to be parameterized, and therefore recommended when only limited unfrozen water observations are available. The water potential–freezing point depression relation (equation (20)) is a good choice in numerical models with coupled soil temperature and soil water simulations, since its parameters (ψ_0 and b) can be obtained from the soil water retention curves. Equation (20) can also couple the thermal transfer equation (equation (4)) with water transfer equation (e.g., Richard's equation) in coupled simulations of soil temperature and moisture regimes. The unfrozen water parameters

(Table 5) derived in this study may provide reference for other modelers with similar site conditions.

[38] (3) Semi-empirical algorithms such as ATIA simulates GTFD reasonably well during thawing periods in permafrost sites or the freezing periods in seasonal frost sites, once the site-calibrated parameter (β) is determined. However, large variation in the β value was found between thawing and freezing, from site to site, and from year to year. Although ATIA serves as a simple tool under equilibrium conditions to quantify the thawing depth in permafrost sites or the freezing depth in seasonal frost sites, it is not recommended to use it in dynamic analyses such as the study of the impacts of climate change.

[39] (4) When driven only by surface forcing and supplied with the best soil moisture inputs and soil texture parameters (HMSA with Run1 and TDSA with Run2), the two analytical algorithms performed only marginally better than the semiempirical algorithm (ATIA). TDSA with both surface and bottom forcing (Run1) improved the GTFD simulations at several sites (Figures 4d, 5d, and 7d), yet their results were still poor compared with those achieved by the numerical algorithms. Unless their original assumptions are met (wet homogenous soil conditions), analytical methods are not preferred for GTFD simulations.

[40] (5) When driven by both surface and bottom temperatures, supplied with observed soil parameters and soil water data, and with optimal model configuration (Run1), numerical algorithms traced observed GTFD evolutions more accurately than the other algorithms at all sites. Even when the observed bottom temperatures were replaced with a simple assumption (zero heat flux at 5-m soil depth), the numerical models, particularly the apparent heat capacity method (FD_AHCP), still achieved comparable results at most sites. However, under the assumption of soil saturation, numerical models failed to perform much better than the semiempirical and analytical algorithms at most sites, indicating accurate representation of soil moisture conditions are critical for numerical GTFD simulations. The AHCP technique in simulating the latent heat consumed (released) during thawing (freezing) performed better and was more stable than the DECP technique conventionally used by many LSMs (e.g., CLASS, *Verseghy* [1991]; IBIS, *Foley et al.* [1996]; CLM, *Dai et al.* [2003]), and should be considered for GTFD simulations.

[41] (6) As demonstrated in many studies [*Smerdon and Stieglitz*, 2006; *Alexeev et al.*, 2007; *Nicolsky et al.*, 2007; *Zhang et al.*, 2007b], model configuration such as resolutions of time step and soil layers and placement of lower soil boundary are critical for numerical thermal algorithms. The configurations presented in Table 7 are only valid for site conditions and applications specified in this study. When applying to different temporal and spatial scales, or different site conditions, alternate configurations should be applied.

[42] (7) The soil surface temperature (T_s) is the most important input for all GTFD algorithms. Although observed T_s values were used in this study, it is very hard to have directly observed T_s as input in spatial or long term studies. To derive T_s from readily available data set such as air temperature and other surface meteorological or reanalysis data is another important process that requires attention in current land surface and hydrological models. It is important to note that many processes such as snow

accumulation and ablation, and the surface energy balance affect the simulation of T_s, which will in turn affect GTFD simulation.

Notation

a, c	empirical coefficients of power function.
b	shape coefficient of the soil water potential–moisture curve.
C	volumetric heat capacity, J m^{-3} °C^{-1}
C_{app}	apparent heat capacity, J m^{-3} °C^{-1}
C_f	soil heat capacity during frozen state, J m^{-3} °C^{-1}
C_u	soil heat capacity during unfrozen state, J m^{-3} °C^{-1}
F	time accumulation of ground surface temperature, d °C.
f_w, f_a, f_s, f_i	influential factor of liquid water, air, soil solids, or ith soil component
g	gravitational acceleration, 9.8 m s^{-2}
g_a, g_c	empirical air pore-shape factors
Hf_s	ground surface heat flux, W m^{-2}
Hf_b	bottom heat flux of soil column, W m^{-2}
$i = 1, N$	all the soil components including air, water, ice, organic, and all kinds of minerals
I_{cov}	convective transport of heat by water flow, W m^{-3}
I_{lat}	latent heat released (consumed) during the phase change of soil moisture, W m^{-3}
K	soil thermal conductivity, W m^{-1} °C^{-1}
K_{dry}	thermal conductivity for dry soil, W m^{-1} °C^{-1}
K_e	Kersten number
K_{sat}	thermal conductivity for saturated soil, W m^{-1} °C^{-1}
K_w, K_a, K_s, K_i	thermal conductivity of liquid water, air, soil solids, or ith soil component, W m^{-1} °C^{-1}
L	latent heat of fusion, 3.34 × 10^8 J m^{-3}
t	time, s
$T, T(z, t)$	soil temperature, °C
T_b	soil bottom temperature, °C
$T_{b,ann}$	annual average soil temperature at bottom layer of observation, °C
T_f	freezing point temperature, °C
T_s	ground surface temperature, °C
$T_{s,ann}$	annual average soil temperature at top layer of observation, °C
$T_{u,l}$	a threshold temperature when unfrozen water content reaches minimum, °C
Z	thawing/freezing depth, m
z	soil depth, m
β	empirical coefficient
θ_0	soil porosity, m^3 m^{-3}
θ	volumetric fraction of total soil moisture, m^3 m^{-3}
θ_{ann}	annual average volumetric fraction of total soil moisture, m^3 m^{-3}
$\theta_w, \theta_a, \theta_s, \theta_i$	volumetric fraction of liquid water, air, soil solids, or ith soil component, m^3 m^{-3}
$\theta_{u,l}$	minimum unfrozen water content, m^3 m^{-3}
ρ	density of ice or water, kg m^{-3}

ρ_b Soil bulk density, kg m^{-3}
ψ soil water potential, m
ψ_0 soil water potential at saturation, m

References

Abbey, F. L., D. M. Gray, D. H. Male, and D. E. L. Erickson (1978), Index models for predicting heat flux to permafrost during thawing conditions, in *Proc. Third International Conference on Permafrost*, pp. 3–9, National Research Council of Canada, Ottawa, Canada.

Alexeev, V. A., D. J. Nicolsky, V. E. Romanovsky, and D. M. Lawrence (2007), An evaluation of deep soil configurations in the CLM3 for improved representation of permafrost, *Geophys. Res. Lett.*, 34, L09502, doi:10.1029/2007GL029536.

Alexiades, V., and A. D. Solomon (1993), *Mathematical Modelling of Melting and Freezing Processes*, 323 pp., Hemisphere, Philadelphia, PA.

Andersland, O. B., and B. Ladanyi (1994), *An Introduction to Frozen Ground Engineering*, 352 pp., Chapman and Hall, Boca Raton, Fla.

Anderson, D. M., and A. R. Tice (1972), Predicting unfrozen water contents in frozen soils from surface area measurements, *Highw. Res. Rec.*, 393, 12–18.

Anisimov, O. A., N. I. Shiklomanov, and F. E. Nelson (2002), Variability of seasonal thaw depth in permafrost regions: A stochastic modeling approach, *Ecol. Modell.*, 153, 217–227.

Becker, F., and Z.-L. Li (1995), Surface temperature and emissivity at various scales: Definition, measurement and related problems, *Remote Sens. Rev.*, 12, 225–253.

Boike, J., K. Roth, and P. P. Overduin (1988), Thermal and hydrologic dynamics of the active layer at a continuous permafrost site (Taymyr Peninsula, Siberia), *Water Resour. Res.*, 34(3), 355–363.

Burn, C. R., and F. E. Nelson (2006), Comment on "A projection of severe near-surface permafrost degradation during the 21st century" by David M. Lawrence and Andrew G. Slater, *Geophys. Res. Lett.*, 33, L21503, doi:10.1029/2006GL027077.

Carey, S. K., and M.-K. Woo (1998), Snowmelt hydrology of two subarctic slopes, southern Yukon, Canada, *Nord. Hydrol.*, 29, 331–346.

Carey, S. K., and M.-K. Woo (1999), Hydrology of two slopes in subarctic Yukon, Canada, *Hydrol. Process.*, 13, 2549–2562.

Carey, S. K., and M.-K. Woo (2001), Slope runoff processes and flow generation in a subarctic, subalpine environment, *J. Hydrol.*, 253, 110–129.

Carey, S. K., and M.-K. Woo (2005), Freezing of subarctic hillslopes, Wolf Creek Basin, Yukon, Canada, *Arct. Antarct. Alp. Res.*, 37, 1–10.

Carlson, H. (1952), Calculation of depth of thaw in frozen ground, in *Frost Action in Soils: A Symposium*, pp. 192–223, United States National Research Council, Highw. Res. Board, Washington, D. C.

Cary, J. W., and H. F. Mayland (1972), Salt and water movement in unsaturated frozen soil, *Soil Sci. Soc. Am. Proc.*, 36, 549–555.

Cherkauer, K. A., and D. P. Lettenmaier (1999), Hydrologic effects of frozen soils in the upper Mississippi River Basin, *J. Geophys. Res.*, 104(D16), 19,599–19,610.

Coll, C., V. Caselles, J. M. Galve, E. Valor, R. Niclo's, J. M. Sa'nchez, and R. Rivas (2005), Ground measurements for the validation of land surface temperatures derived from AATSR and MODIS data, *Remote Sens. Environ.*, 97, 288–300.

Dai, Y., et al. (2003), The Common Land Model, *Bull. Am. Meteorol. Soc.*, 84, 1013–1023.

de Vries, D. A. (1963), Thermal properties of soil, in *Physics of Plant Environment*, edited by W. R. van Dijk, pp. 210–235, North Holland Publishing, Amsterdam.

Delisle, G. (2007), Near-surface permafrost degradation: How severe during the 21st century?, *Geophys. Res. Lett.*, 34, L09503, doi:10.1029/2007GL029323.

Farouki, O. T. (1986), *Thermal Properties of Soils*. 136 pp., Trans. Tech. Publications, Clausthal-Zellerfeld, Germany.

Foley, J. A., I. C. Prentice, N. Ramankutty, S. Levis, D. Pollard, S. Sitch, and A. Haxeltine (1996), An integrated biosphere model of land surface processes, terrestrial carbon balance, and vegetation dynamics, *Global Biogeochem. Cycles*, 10(4), 603–628.

Fox, J. D. (1992), Incorporating freeze-thaw calculations into a water balance model, *Water Resour. Res.*, 28(9), 2229–2244.

Fuchs, M., G. S. Campbell, and R. I. Papendick (1978), An analysis of sensible and latent heat flow in a partially frozen unsaturated soil, *Soil Sci. Soc. Am. J.*, 42(3), 379–385.

Goodrich, L. E. (1978), Efficient numerical technique for one dimensional geothermal problems with phase change, *Int. J. Heat Mass Transfer*, 21, 615–621.

Goodrich, L. E. (1982a), *An Introductory Review of Numerical Methods for Ground Thermal Regime Calculations*. 33 pp., DBR Paper No. 1061, Division of Building Research, National Research Council of Canada, Ottawa, ON, Canada.

Goodrich, L. E. (1982b), The influence of snow cover on the ground thermal regime, *Can. Geotech. J.*, 19, 421–432.

Gu, S., Y. Tang, X. Cui, T. Kato, M. Du, Y. Li, and X. Zhao (2005), Energy exchange between the atmosphere and a meadow ecosystem on the Qinghai–Tibetan Plateau, *Agric. For. Meteorol.*, 129, 175–185.

Hayashi, M., N. Goeller, W. L. Quinton, and N. Wright (2007), A simple heat-conduction method for simulating the frost-table depth in hydrological models, *Hydrol. Process.*, 21(19), 2610–2622.

Hinkel, K. M., and J. R. J. Nicholas (1995), Active layer thaw rate at a boreal forest site in central Alaska, USA, *Arct. Alp. Res.*, 27(1), 72–80.

Hinkel, K. M., and S. I. Outcalt (1994), Identification of heat-transfer processes during soil cooling, freezing and thaw in Central Alaska, *Permafrost Periglac. Process.*, 5, 217–235.

Hinzman, L. D., D. J. Goering, and D. L. Kane (1998), A distributed thermal model for calculating soil temperature profiles and depth of thaw in permafrost regions, *J. Geophys. Res.*, 103(D22), 28,975–28,991.

Johansen, O. (1975), Thermal conductivity of soils, Ph.D. thesis, Institute for Kjoleteknik, Trondheim-NTH, Norway. (CRREL Draft Translation 637, 1977), ADA 044002.

Jumikis, A. R. (1977), *Thermal Geotechnics*, 375 pp., Rutgers Univ. Press, Piscataway, N. J.

Kade, A., V. E. Romanovsky, and D. A. Walker (2006), The *N*-factor of nonsorted circles along a climate gradient in Arctic Alaska, *Permafrost Periglac. Process.*, 17, 279–289.

Kane, D. L., K. M. Hinkel, D. J. Goering, L. D. Hinzman, and S. I. Outcalt (2001), Non-conductive heat transfer associated with frozen soils, distribution in Canada during the 21st century under scenarios of climate change, *Global Planet. Change*, 29, 275–292.

Kersten, M. S. (1959), Frost penetration: Relationship to air temperature and other factors, *Highw. Res. Board, Bull.*, 225, 45–80.

Klene, A. E., F. E. Nelson, N. I. Shiklomanov, and K. M. Hinkel (2001), The n-factor in natural landscapes: Variability of air and soil-surface temperatures, Kuparuk River Basin, Alaska, USA, *Arct. Antarct. Alp. Res.*, 33, 140–148.

Koopmans, R. W. R., and R. D. Miller (1966), Soil freezing and soil water characteristic curves, *Soil Sci. Soc. Am. Proc.*, 22, 278–281.

Koren, V., J. Schaake, K. Mitchell, Q.-Y. Duan, F. Chen, and J. M. Baker (1999), A parameterization of snowpack and frozen ground intended for NCEP weather and climate models, *J. Geophys. Res.*, 104(D16), 19,569–19,585.

Lachenbruch, A. H., J. H. Sass, B. V. Marshall, and T. H. Moses Jr. (1982), Permafrost, heat flow and geothermal regime at Prudhoe Bay, Alaska, *J. Geophys. Res.*, 87(B11), 9301–9316.

Lawrence, D. M., and A. G. Slater (2005), A projection of severe near surface permafrost degradation during the 21st century, *Geophys. Res. Lett.*, 32, L24401, doi:10.1029/2005GL025080.

Li, X., and T. Koike (2003), Frozen soil parameterization in SiB2 and its validation with GAME-Tibet observations, *Cold Reg. Sci. Technol.*, 36(1–3), 165–182.

Ling, F., and T. Zhang (2004), A numerical model for surface energy balance and thermal regime of the active layer and permafrost containing unfrozen water, *Cold Reg. Sci. Technol.*, 38, 1–15.

Lunardini, V. J. (1981), *Heat Transfer in Cold Climates*, 731 pp., Van Nostrand Reinhold, New York.

Luo, L., et al. (2003), Effects of frozen soil on soil temperature, spring infiltration, and runoff: Results from the PILPS 2 (d) experiment at Valdai, Russia, *J. Hydrometeorol.*, 4, 334–351.

McCauley, C. A., D. M. White, M. R. Lilly, and D. M. Nyman (2002), A comparison of hydraulic conductivities, permeabilities and infiltration rates in frozen and unfrozen soils, *Cold Reg. Sci. Technol.*, 34, 117–125.

McNamara, J. P., D. L. Kane, and L. D. Hinzman (1998), An analysis of stream flow hydrology in the Kuparuk River Basin, Arctic Alaska: A nested watershed approach, *J. Hydrol.*, 206, 39–57.

Metcalfe, R. A., and J. M. Buttle (1999), Semi-distributed water balance dynamics in a small boreal forest basin, *J. Hydrol.*, 226, 66–87.

Nakano, Y., and J. Brown (1972), Mathematical modeling and validation of the thermal regimes in tundra soils, Barrow, Alaska, *Arct. Alp. Res.*, 4(1), 19–38.

Nelson, F. E., and S. I. Outcalt (1987), A computational method for prediction and regionalization of permafrost, *Arct. Alp. Res.*, *19*(3), 279–288.

Nelson, F. E., N. I. Shiklomanov, G. Mueller, K. M. Hinkel, D. A. Walker, and J. G. Bockheim (1997), Estimating active layer thickness over a large region: Kuparuk river basin, Alaska, USA, *Arct. Alp. Res.*, *29*(4), 367–378.

Nicolsky, D. J., V. E. Romanovsky, V. A. Alexeev, and D. M. Lawrence (2007), Improved modeling of permafrost dynamics in Alaska with CLM3, *Geophys. Res. Lett.*, *34*, L08501, doi:10.1029/2007GL029525.

Niu, G.-Y., and Z.-L. Yang (2006), Effects of frozen soil on snowmelt runoff and soil water storage at a continental scale, *J. Hydrometeorol.*, *7*, 937–952.

Osterkamp, T. E. (1987), Freezing and thawing of soils and permafrost containing unfrozen water or brine, *Water Resour. Res.*, *23*(12), 2279–2285.

Osterkamp, T. E., and V. E. Romanovsky (1997), Freeze-up of the active layer on the coastal plain in the Alaskan Arctic, *Permafrost Periglac. Process.*, *8*, 23–44.

Outcalt, S. I., F. E. Nelson, and K. M. Hinkel (1990), The zero-curtain effect: Heat and mass transfer across an isothermal region in freezing soil, *Water Resour. Res.*, *26*(7), 1509–1516.

Overduin, P. P., D. L. Kane, and W. K. P. van Loon (2006), Measuring thermal conductivity in freezing and thawing soil using the soil temperature response to heating, *Cold Reg. Sci. Technol.*, *45*, 8–22.

Pitman, A. J., A. G. Slater, C. E. Desborough, and M. Zhao (1999), Uncertainty in the simulation of runoff due to the parameterization of frozen soil moisture using the Global Soil Wetness Project methodology, *J. Geophys. Res.*, *104*(D14), 16,879–16,888.

Quinton, W. L., and D. M. Gray (2001), Estimating subsurface drainage from organic-covered hillslopes underlain by permafrost: Toward a combined heat and mass flux model, in *Soil-Vegetation-Atmosphere Transfer Schemes and Large-Scale Hydrological Models*, Proceedings of a symposium held during the Sixth IAHS Scientific Assembly at Maastricht, Netherlands, July 2001, pp. 333–341, IAHS Publ. 270, IAHS Press, Wallingford, U.K.

Quinton, W. L., T. Shirazi, S. K. Carey, and J. W. Pomeroy (2005), Soil water storage and active-layer development in a sub-alpine tundra hillslope, southern Yukon Territory, Canada, *Permafrost Periglac. Process.*, *16*, 369–382.

Riseborough, D. W. (2004), Exploring the parameters of a simple model of the permafrost–climate relationship, 328 pp., PhD thesis, Carleton Univ., Ottawa, Canada.

Romanovsky, V. E., and T. E. Osterkamp (1997), Thawing of the active layer on the coastal plain of the Alaskan Arctic, *Permafrost Periglac. Process.*, *8*, 1–22.

Romanovsky, V. E., and T. E. Osterkamp (2000), Effects of unfrozen water on heat and mass transport processes in the active layer and permafrost, *Permafrost Periglac. Process.*, *11*, 219–239.

Romanovsky, V. E., T. E. Osterkamp, and N. S. Duxbury (1997), An evaluation of three numerical models used in simulations of the active layer and permafrost temperature regimes, *Cold Reg. Sci. Technol.*, *26*, 195–203.

Shoop, S. A., and S. R. Bigl (1997), Moisture migration during freeze and thaw of unsaturated soils: Modeling and large scale experiments, *Cold Reg. Sci. Technol.*, *25*, 33–45.

Slater, A. G., A. J. Pitman, and C. E. Desborough (1998), Simulation of freeze-thaw cycles in general circulation model land surface scheme, *J. Geophys. Res.*, *103*(D10), 11,303–11,312.

Smerdon, J. E., and M. Stieglitz (2006), GRL, Simulating heat transport of harmonic temperature signals in the Earth's shallow subsurface: Lower boundary sensitivities, *Geophys. Res. Lett.*, *33*, L14402, doi:10.1029/2006GL026816.

Smirnova, T. G., J. M. Brown, S. G. Benjamin, and D. Kim (2000), Parameterization of cold-season processes in the MAPS land-surface scheme, *J. Geophys. Res.*, *105*(D3), 4077–4086.

Stefan, J. (1890), Über die Theorie der Eisbildung, Insbesondere uberdie Eisbildung im Polarmeere, *Sitzungsberichte der mathematisch-Naturwissenschaftlichen Classe der Kaiserlichen Akademie der Wissenschaften*, 98 (IIa), 965–983.

Stevens, M. B., J. E. Smerdon, J. F. Gonza'lez-Rouco, M. Stieglitz, and H. Beltrami (2007), Effects of bottom boundary placement on subsurface heat storage: Implications for climate model simulations, *Geophys. Res. Lett.*, *34*, L02702, doi:10.1029/2006GL028546.

Sushama, L., R. Laprise, and M. Allard (2006), Modeled current and future soil thermal regime for North East Canada, *J. Geophys. Res.*, *111*, D18111, doi:10.1029/2005JD007027.

Sushama, L., R. Laprise, D. Caya, D. Verseghy, and M. Allard (2007), An RCM projection of soil thermal and moisture regimes for North American permafrost zones, *Geophys. Res. Lett.*, *34*, L20711, doi:10.1029/2007GL031385.

Tarnawski, V. R., and B. Wagner (1992), A new computerized approach to estimating the thermal properties of unfrozen soils, *Can. Geotech. J.*, *29*, 714–720.

Tarnawski, V. R., and B. Wagner (1993), Modeling the thermal conductivity of frozen soils, *Cold Reg. Sci. Technol.*, *22*, 19–31.

Torrance, J. K., and F. J. Schellekens (2006), Chemical factors in soil freezing and frost heave, *Polar Rec.*, *42*(220), 33–42.

Van Wijk, W. R. (1963), *Physics of Plant Environment*, 166 pp., North-Holland, New York.

Verseghy, D. L. (1991), CLASS—A Canadian land surface scheme for GCMs, I. Soil model, *Int. J. Climatol.*, *11*, 111–113.

Williams, P. J., and M. W. Smith (1989), *The Frozen Earth: Fundamentals of Geocryology*, 306 pp., Cambridge Univ. Press, New York.

Woo, M.-K. (1976), Hydrology of a small Canadian High Arctic basin during the snowmelt period, *Catena*, *3*, 155–168.

Woo, M.-K. (1986), Permafrost hydrology in North America, *Atmosphere-Ocean*, *24*, 201–234.

Woo, M.-K., A. M. Arain, M. Mollinga, and S. Yi (2004), A two-directional freeze and thaw algorithm for hydrologic and land surface modelling, *Geophys. Res. Lett.*, *31*, L12501, doi:10.1029/2004GL019475.

Yalamanchili, R. V. S., and S. C. Chu (1973), Stability and oscillation characteristics of finite-element, finite-difference, and weighted-residuals methods for transient two-dimensional heat conduction in solid, *Heat Transfer, J.*, Transactions of the ASME Series C95, 2, 235–239.

Yi, S., A. M. Arain, and M.-K. Woo (2006), Modifications of a land surface scheme for improved simulation of ground freeze-thaw in northern environments, *Geophys. Res. Lett.*, *33*, L13501, doi:10.1029/2006GL026340.

Zhang, Z., D. L. Kane, and L. D. Hinzman (2000), Development and application of a spatial-distributed Arctic hydrological and thermal process model, *Hydrol. Process.*, *14*, 1591–1611.

Zhang, Y., W. Chen, and J. Cihlar (2003), A process based model for quantifying the impact of climate change on permafrost thermal regimes, *J. Geophys. Res.*, *108*(D22), 4695, doi:10.1029/2002JD003354.

Zhang, Y., W. Chen, and D. W. Riseborough (2007a), Transient projections of permafrost distribution in Canada during the 21st century under scenarios of climate change, *Global Planet. Change*, doi:10.1016/j.gloplacha.2007.05.003.

Zhang, Y., S. Wang, A. G. Barr, and T. A. Black (2007b), Impact of snow cover on soil temperature and its simulation in a boreal aspen forest, *Cold Reg. Sci. Technol.*, doi:10.1016/j.coldregions.2007.07.001.

Zhao, L., and D. M. Gray (1997), A parametric expression for estimating infiltration into frozen soils, *Hydrol. Process.*, *11*, 1761–1775.

————————————

S. K. Carey and Y. Zhang, Department of Geography and Environmental Studies, Carleton University, B349 Loed Building, 1125 Colonel By Drive, Ottawa, ON K1S 5B6, Canada. (yinsou_zhang@carleton.ca)

W. L. Quinton, Cold Regions Research Centre, Wilfrid Laurier University, Waterloo, ON, Canada.